Supplement of Nonlin. Processes Geophys., 28, 121–134, 2021
https://doi.org/10.5194/npg-28-121-2021-supplement

Nonlinear Processes in Geophysics
Open Access

Supplement of

Application of Lévy processes in modelling (geodetic) time series with mixed spectra

Jean-Philippe Montillet et al.

Correspondence to: Jean-Philippe Montillet (jpmontillet@segal.ubi.pt)

S3.1. Geophysical model and ML Estimator

Following Section 2.1 in order to obtain the residual time series $x(t)$ (t the epoch), we subtract the functional model $s_0(t)$ from the GNSS observations $s(t)$ (see Eq. (1)). The functional model of the geophysical signals is based on the polynomial trigonometric method (Li et al. , 2000; Williams , 2003; Tregoning and Watson , 2009).

$$s_0(t) = at + b + \sum_{j=1}^{N} (c_j \cos(d_j t) + e_j \sin(d_j t)) \tag{S1.1}$$

with $s_0(t)$ the sum of the tectonic rate (with coefficient a and b) and the seasonal signal (sum of $\cos$ and $\sin$ functions with coefficients c_j and e_j). Note that d_j is equal to $2\pi j/N$, and N can be equal up to 7 (He et al. , 2017). One can also add a Heaviside step function at time t_i in order to estimate the amplitude of an offsets (see appendix). It should be emphasised that the geophysical model is selected based on the surrounding geodynamical activity around the GNSS stations (Montillet and Bos , 2019). Finally, the residual signal is considered to be the remaining geophysical signals (i.e. seasonal component and tectonic rate) not completely estimated due to the mismodelling of the stochastic properties of the time series and other small amplitude (i.e. sub-millimeter) short-time duration transient signals (i.e. local signals, subsidence, ...) (Bos et al. , 2013; Montillet et al. , 2015; Herring et al. , 2016; He et al. , 2017).

In this study, the Hector software is used to estimate jointly the functional and stochastic models in order to produce the residual time series as described in Section 2.4. The software is based on a maximum likelihood estimator (MLE). To recall Eq. (3), the log-likelihood for a time series of length L is :

$$\ln(Lo) = -\frac{1}{2}\left[L\ln(2\pi) + \ln(\det(\boldsymbol{C})) + (\boldsymbol{s} - \boldsymbol{A}\boldsymbol{z})^T \boldsymbol{C}^{-1} (\boldsymbol{s} - \boldsymbol{A}\boldsymbol{z})\right] \tag{S1.2}$$

The covariance matrix $\boldsymbol{C}$ is assumed to be known. The term $(\boldsymbol{s} - \boldsymbol{A}\boldsymbol{z})$ represents the observations minus the fitted model. $(\boldsymbol{A}\boldsymbol{z})$ is the matrix notation of $s_0(t)$. The last term is a quadratic function, weighted by the inverse of matrix $\boldsymbol{C}$.

Now let us compute the derivative of $\ln(Lo)$:

$$\frac{d\ln(Lo)}{d\boldsymbol{z}} = \boldsymbol{A}^T \boldsymbol{C}^{-1} \boldsymbol{s} - \boldsymbol{A}^T \boldsymbol{C}^{-1} (\boldsymbol{A}\boldsymbol{z}) \tag{S1.3}$$

The minimum of $\ln(Lo)$ occurs when this derivative is zero. Thus:

$$\boldsymbol{A}^T \boldsymbol{C}^{-1} (\boldsymbol{A}\boldsymbol{z}) = \boldsymbol{A}^T \boldsymbol{C}^{-1} \boldsymbol{s} \;\rightarrow\; \boldsymbol{z} = \left(\boldsymbol{A}^T \boldsymbol{C}^{-1} \boldsymbol{A}\right)^{-1} \boldsymbol{A}^T \boldsymbol{C}^{-1} \boldsymbol{s} \tag{S1.4}$$

This is the weighted least-squares equation to estimate the parameters $\boldsymbol{z}$. Most derivations of this equation focus on the minimisation of the quadratic cost function. However, here we highlight the fact that for observations that contain Gaussian multivariate noise, the weighted least-squares estimator is a maximum likelihood estimator (MLE). Therefore, the Hector software estimates the functional and stochastic parameters via the MLE. Note that in our case $\boldsymbol{C}$ is not a constant, because we assume that the time series contain white and coloured noise. In fact $\boldsymbol{C}$ is equal to the covariance matrix $E\{\mathbf{n}^T\mathbf{n}\}$ in Section 2.1. Thus, the expression of $\boldsymbol{C}$ changes depending on the selection of the stochastic noise model (i.e. Flicker + White noise, Power-law + white noise) discussed in Section 2. Further assumptions (i.e. matrix computation) to increase the computational speed can be found in (Bos et al. , 2013) and (Montillet and Bos , 2019). Finally, the Gaussian multivariate noise model (or Gauss-Markov assumption) holds with the additional assumption that the coloured noise is slowly varying which means that 1/ the noise is non-stationary around the mean, and 2/ no intermittency in the time series, i.e. no events creating short high bursts or sudden large deviations for the mean.

S3.2. Relationship between the FARIMA, ARMA and fBm

Following Granger and Joyeux (1980), Panas (2001) and Pipiras and Taqqu (2017), a time series (e.g., $\mathbf{x}$) follows an FARIMA (p,d,q) process if it can be defined by

$$\begin{aligned}
\Psi_p(Z)x(t) &= \Theta_k(Z)(1-Z)^{-d}b(t) \\
\Psi_p(Z) &= 1-a_1*Z-a_2*Z^2-...-a_p*Z^p \\
\Theta_q(Z) &= 1+b_1*Z+b_2*Z^2+...+b_k*Z^q \\
(1-Z)^{-d} &= \sum_{j=0}^{\infty}\frac{\Gamma(j+d)}{\Gamma(j+1)\Gamma(d)}*Z^j
\end{aligned} \tag{S1.5}$$

where $E\{\mathbf{b}\}$ equal zero and $\sigma_b^2<\infty$. Z is the backshift operator applied to $x\ (t)$ and $b\ (t)$, respectively. The properties of the FARIMA model are presented by Granger and Joyeux (1980): i) if the roots of $\Phi_p(Z)$ and $\Theta_q(Z)$ are outside the unit circle and $d<|0.5|$, then $\mathbf{x}$ is both stationary and invertible; ii) if $0<d<0.5$ the FARIMA model is capable of generating stationary series which are persistent. In this case the process displays long-memory characteristics, with an algebraic autocorrelation decay to zero; iii) if $d\geq 0.5$ the process is non-stationary ; iv) when d equal to 0 it is an ARMA process exhibiting short memory; v) when $-0.5\leq d<0$ the FARIMA process is said to exhibit intermediate memory or anti-persistence. This is very similar to the description of the Hurst parameter in the fBm model. Note that one can underline the relationship between d and H such as $H=d+0.5$, well-known in financial time series analysis in the presence of aggregation processes (Panas , 2001). The fBm can be defined by its integral representation (see previous section) or the aggregation of fractional Gaussian noise (Taqqu et al. , 1995).

S3.3. fBm and fLsm: integral representation and discussion

The fractional Brownian motion (fBm) $\{B_H(t)\}_{t\geq 0}$ has the integral representation:

$$B_H(t)=\int_{-\infty}^{\infty}\left((t-u)_+^{H-\frac{1}{2}}-(-u)_+^{H-\frac{1}{2}}\right)dB(u) \tag{S1.6}$$

where $x_+=max(x,0)$ and $B(u)$ is a Brownian motion (Bm). It is H-self-similar with stationary increments and it is the only Gaussian process with such properties for $0<H<1$ (Samorodnitsky and Taqqu , 1994). It is worth mentioning that a damped version of the fBm exists and known as the Matérn process, defined having a sloped spectrum that matches fBm at high frequencies and taking on a constant value in the vicinity of zero frequency (Lilly et al. , 2017). However, this process is out of the scope of this study.

From Weron et al. (2005), the fractional Lévy stable motion (fLsm) can be defined with the process $\{Z_\alpha^H(t)\}$ (with t in $\mathbb{R}$) by the following integral representation:

$$\begin{aligned}
Z_\alpha^H(t) &= \int_{-\infty}^{\infty}\left((t-u)_+^{H-\frac{1}{\alpha}}-(-u)_+^{H-\frac{1}{\alpha}}\right)dZ_\alpha(u) \\
&= \int_{-\infty}^{\infty}f_t(u)dZ_\alpha(u)
\end{aligned} \tag{S1.7}$$

where $Z_\alpha(u)$ is a symmetric Lévy-stable motion (Lsm). The integral is well defined for $0<H<1$ and $0<\alpha\leq 2$ as a weighted average of the Lévy stable motion $Z_\alpha(u)$ over the infinite past with the weight given by the above integral kernel denoted by

$f_t(u)$. The process $Z_\alpha^H(t)$ is H-self-similar and has stationary increments. H-self-similarity follows from the above integral representation and the fact that the kernel $f_t(u)$ is r-self-similar with $r = H - 1/\alpha$, when the integrator $Z_\alpha(u)$ is $1/\alpha$-self-similar. This implies the following important relation:

$$H = r + 1/\alpha \tag{S1.8}$$

The representation of fLsm in Eq. (S1.7) is similar to the representation (S1.6) of the fractional Brownian motion. Therefore fLsm reduces to the fractional Brownian motion if one sets $\alpha = 2$. When we put $H = 1/\alpha$ we obtain the Lévy α-stable motion which is an extension of the Brownian motion to the α-stable case. At the contrary to the Gaussian case ($\alpha = 2$) the Lévy α-stable motion ($0 < \alpha < 2$) is not the only $1/\alpha$-self-similar Lévy α-stable process with stationary increments. This is true for $0 < \alpha < 1$ only (Weron et al. , 2005). Note that this definition of the Fractional Lévy process is different from Benassi et al. (2004), which is not a self-similar process. Finally, another type of processes worth mentioning is the Cauchy-class of processes, which consist of the stationary Gaussian random processes defined by a correlation function which depends on the Hurst parameter which can be seen as the generalization of some stochastic models (Gneiting and Schlather , 2004).

S3.4. Some Considerations on the Simulations of the Mixed Noise in the GNSS time Series

This section recalls one way to simulate the coloured noise in the GNSS time series following Montillet and Bos (2019). Granger and Joyeux (1980) and Hosking (1981) demonstrated that power-law noise can be achieved using fractional differencing of Gaussian noise:

$$(1-B)^{-K/2}\boldsymbol{v} = \boldsymbol{w} \tag{S1.9}$$

where B is the backward-shift operator ($Bv_i = v_{i-1}$) and $\boldsymbol{v}$ a vector with independent and identically distributed (IID) Gaussian noise. Hosking and Granger used the parameter d for the fraction $-K/2$ which is more concise when one focuses on the fractional differencing aspect. However, in Geodesy the spectral index K is used in the equations. Hosking's definition of the fractional differencing is:

$$\begin{aligned}(1-B)^{-K/2} &= \sum_{i=0}^{\infty} \binom{-K/2}{i}(-B)^i \\ &= 1 - \frac{K}{2}B - \frac{1}{2}\frac{K}{2}(1-\frac{K}{2})B^2 + \ldots \\ &= \sum_{i=0}^{\infty} h_i \end{aligned} \tag{S1.10}$$

The coefficients h_i can be viewed as a filter that is applied to the independent white noise. These coefficients can be conveniently computed using the following recurrence relation (Kasdin , 1995):

$$\begin{aligned} h_0 &= 1 \\ h_i &= (i - \frac{K}{2} - 1)\frac{h_{i-1}}{i} \quad \text{for } i > 0 \end{aligned} \tag{S1.11}$$

One can see that for increasing i, the fraction $(i - K/2 - 1)/i$ is slightly less than 1. Thus, the coefficients h_i only decrease very slowly to zero. This implies that the current noise value w_i depends on many previous values of $\boldsymbol{v}$. In other words, the noise has a long-memory. Eq. (S1.11) also shows that when the spectral index $K = 0$, then all coefficients h_i are zero except for h_0. This implies that there is no temporal correlation between the noise values. One normally assumes that $v_i = 0$ for $i < 0$. With this assumption, the unit covariance between w_k and w_l with $l > k$ is:

$$C(w_k, w_l) = \sum_{i=0}^{k} h_i h_{i+(l-k)} \tag{S1.12}$$

Since $K = 0$ produces an identity matrix, the associated white noise covariance matrix is represented by the unit matrix $\boldsymbol{I}$. The general power-law covariance matrix is represented by matrix $\boldsymbol{J}$ following Williams (2003). It is a widely used combination of noise models to describe the noise in GNSS time series (Williams et al. , 2004). Besides the parameters of the linear model (i.e. the functional model), maximum likelihood estimation can be used to also estimate the parameters K, σ_{pl} and σ_{wn}. This approach has been implemented various software packages including Hector (Bos et al. , 2013).

We assumed that $v_i = 0$ for $i < 0$ which corresponds to no noise before the first observation. This is an important assumption that has been introduced for a practical reason. For a spectral index K smaller than -1, the noise becomes non-stationary. Most GNSS time series contain flicker noise which is just non-stationary. Using the assumption of zero noise before the first observation, the covariance matrix slowly grows over time but always remains finite.

S3.5. Additional Tables and Figures

Table S6.1. Statistics on the Error when fitting the ARMA and FARIMA model to the residual time series for each coordinate of the stations $ALBH$, $DRAO$ and $ASCO$ based on the $FN + WN$ stochastic noise model. Correlation between the distribution of the residuals and the Normal (*Corr. Normal*) and the Lévy α-stable distributions (*Corr. Lévy*). The last column is the Anderson-Darling test. [*Lévy*] or [*Normal*] means the type of distribution uses as the null hypothesis (1 not rejected, 0 rejected).

DRAO	*(err. in mm) ARMA*	*(err. in mm) FARIMA*	*Corr. Normal*	*Corr. Lévy*	AD test [*Lévy*]	AD test [*Normal*]
East	1.07 ± 0.01	1.00 ± 0.02	0.95	0.95	1	1
North	1.02 ± 0.02	1.32 ± 0.07	0.96	0.98	1	1
Up	2.33 ± 0.18	2.20 ± 0.32	0.94	0.96	1	1
ASCO						
East	0.77 ± 0.01	0.75 ± 0.07	0.95	0.96	1	1
North	0.85 ± 0.03	0.74 ± 0.05	0.94	0.96	1	1
Up	2.18 ± 0.14	2.51 ± 0.21	0.93	0.94	1	1
ALBH						
East	0.97 ± 0.04	0.86 ± 0.06	0.95	0.95	1	1
North	1.52 ± 0.08	1.08 ± 0.10	0.96	0.95	1	1
Up	3.83 ± 0.21	3.32 ± 0.15	0.93	0.95	1	0

Figure S5.1. Percentage of variations of the estimated parameters included in the stochastic and functional models when varying the length of the daily position GNSS time series corresponding to the stations $DRAO$, $ASCO$ and $ALBH$. The statistics are estimated over the East, North and Up coordinates

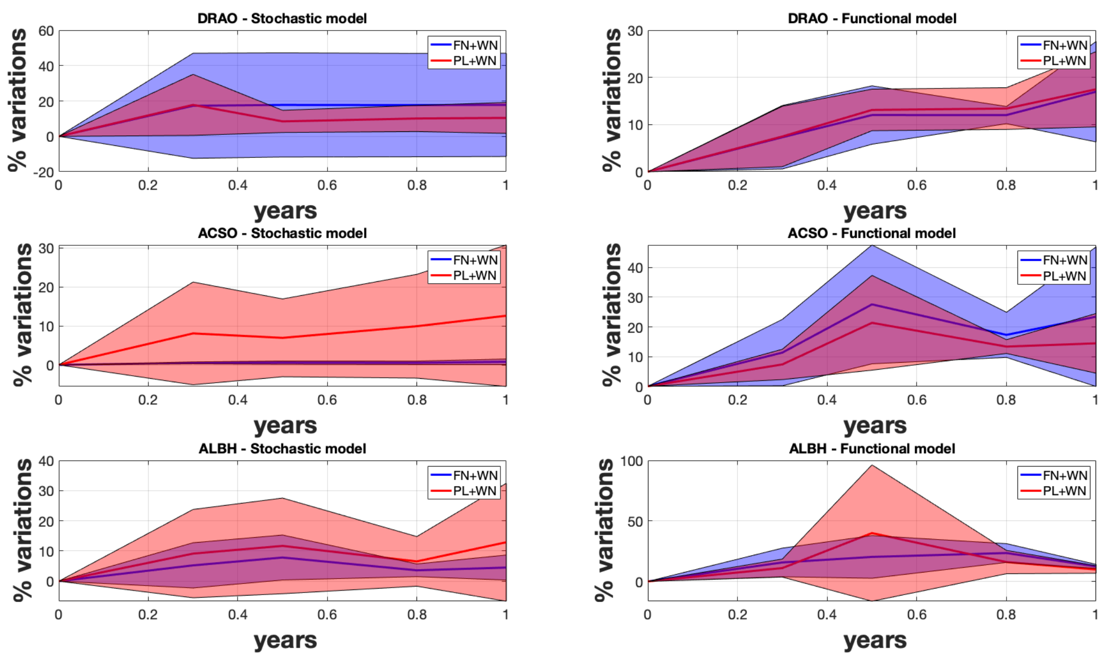

Figure S5.2. GNSS time series for the $DRAO$ station (North coordinate) with the $FN + WN$ model. A/ the time series together with the functional model, B/ the power-spectrum, C/ Residual time series with Lévy α-stable distribution, D/ cumulative density function residual time series and Lévy α-stable distribution (Corr. Lévy $= 0.98$), E/ Residual time series with Normal distribution, F/ cumulative density function of the residual time series and Normal distribution (Corr. Norm. $= 0.96$).

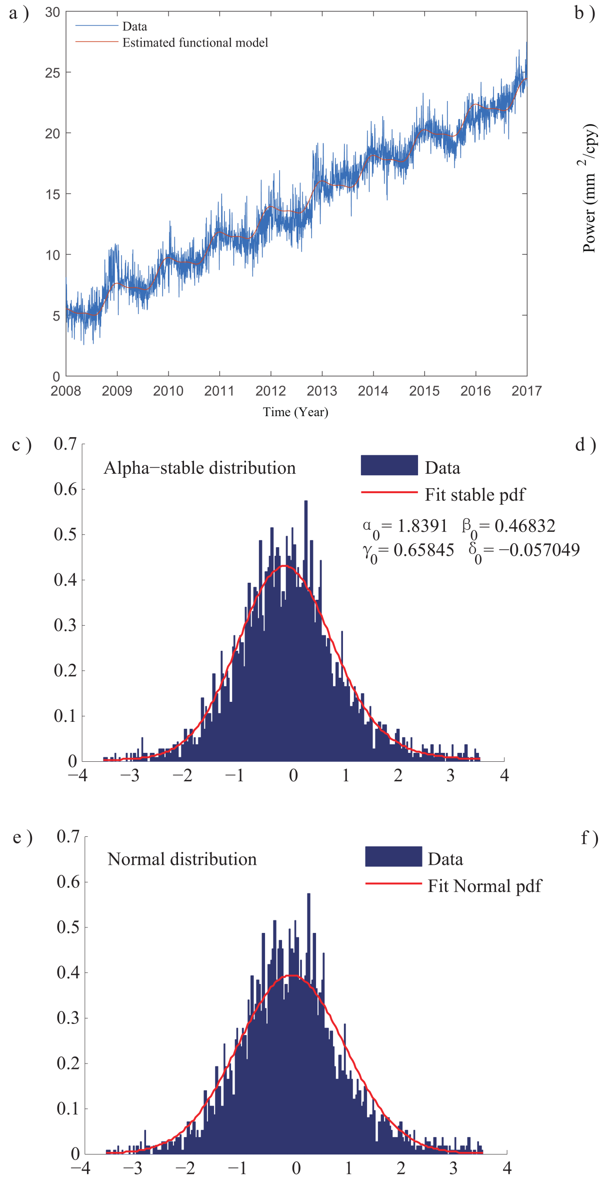

Figure S5.3. GNSS time series for the $ALBH$ station (East coordinate) with the $PL + WN$ model. A/ the time series together with the functional model, B/ the power-spectrum, C/ Residual time series with Lévy α-stable distribution, D/ cumulative density function residual time series and Lévy α-stable distribution (Corr. Lévy $= 0.98$), E/ Residual time series with Normal distribution, F/ cumulative density function of the residual time series and Normal distribution (Corr. Norm. $= 0.98$).

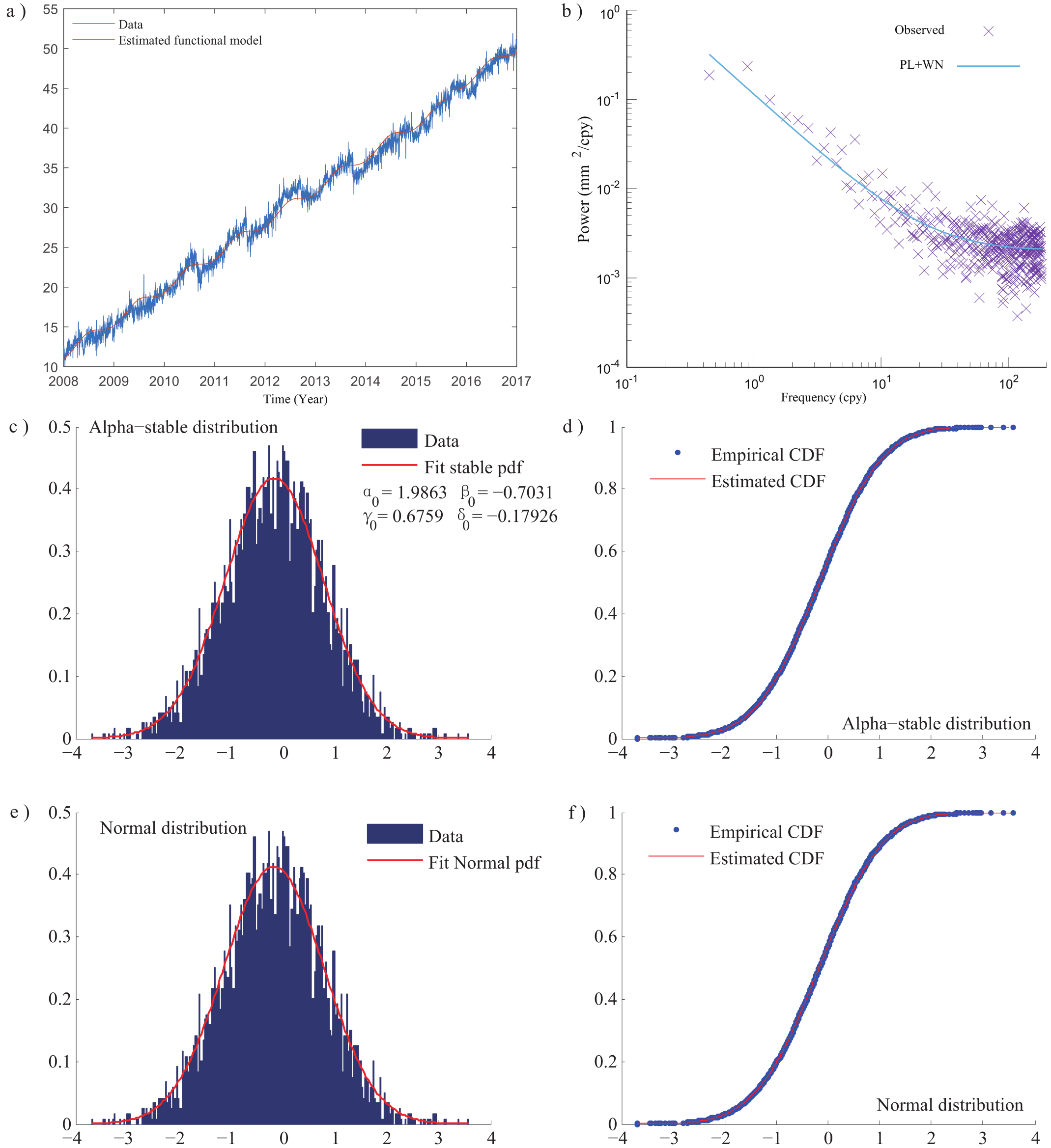

Figure S5.4. GNSS time series for $DRAO$ (Up coordinate) with the $PL+WN$ model. A/ the time series together with the functional model, B/ the power-spectrum, C/ Residual time series with Lévy α-stable distribution, D/ cumulative density function residual time series and Lévy α-stable distribution(Corr. Lévy $= 0.98$), E/ Residual time series with Normal distribution, F/ cumulative density function of the residual time series and Normal distribution(Corr. Norm. $= 0.97$).

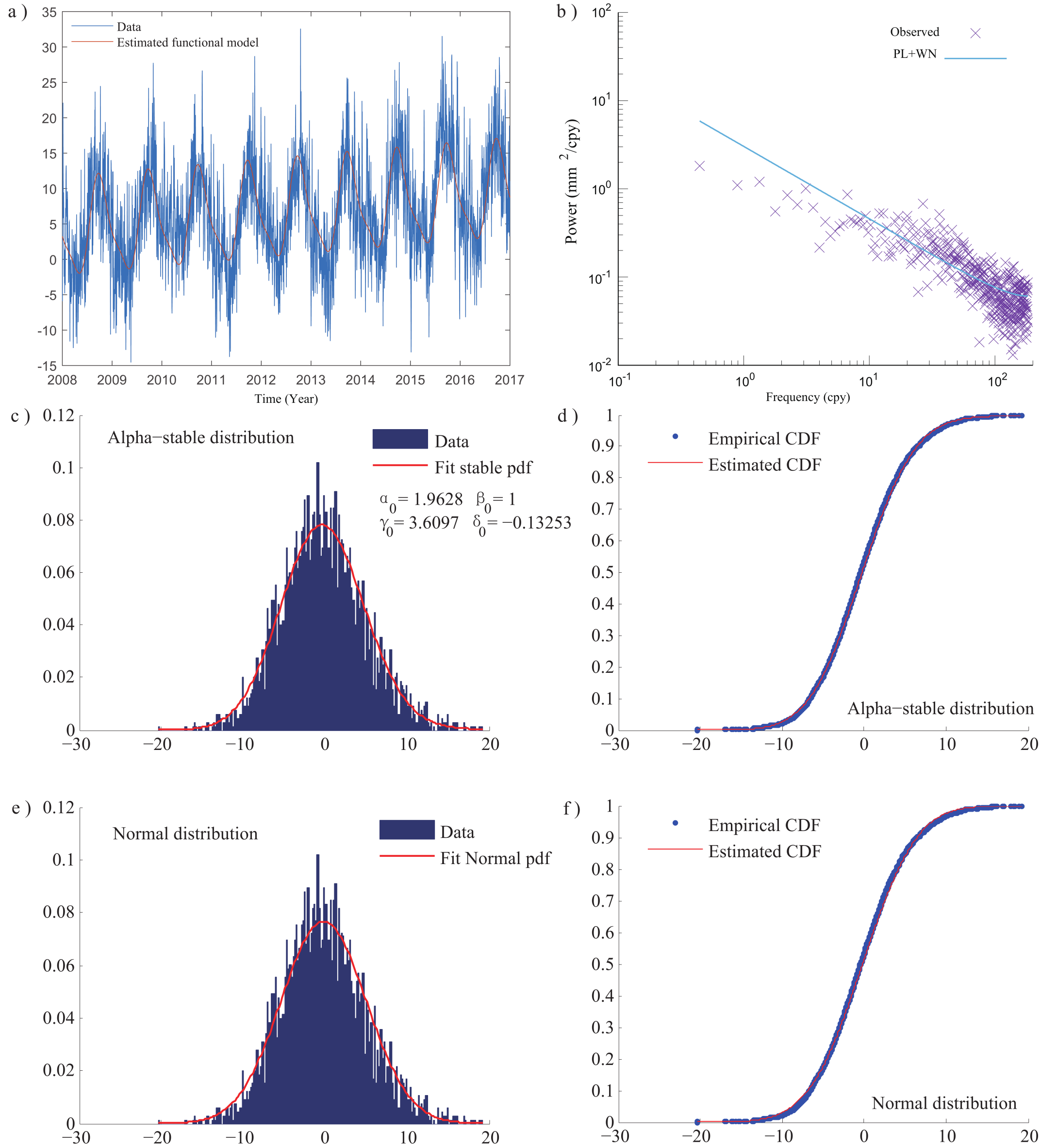

References

Benassi, A., Cohen, S., and Istas, J.: On roughness indices for fractional fields. Bernoulli, 10(2), 357-373, 2004.

Bos, M.S., Fernandes, R.M.S., Williams, S.D.P., Bastos, L.: Fast error analysis of continuous GNSS observations with missing data. J. Geod., 87, 351–360, https://doi.org/10.1007/s00190-012-0605-0, 2013.

Granger, C.W., Joyeux, R. : An introduction to long-memory time series models and fractional differencing. J. Time Ser. Anal., 1, 15-29, https://doi.org/10.1111/j.1467-9892.1980.tb00297.x, 1980.

Gneiting, T., Schlather, M.: Stochastic Models That Separate Fractal Dimension and the Hurst Effect. SIAM Rev., 46(2), 269-282, https://doi.org/10.1137/S0036144501394387, 2004.

He, X., Montillet, J.-P., Fernandes, R.M.S., Bos, M.S., Yu, K., Hua, X., Jiang, W.: Review of current GPS methodologies for producing accurate time series and their error sources. J. Geodyn., 106, https://doi.org/10.1016/j.jog.2017.01.004, 2017.

Herring, T.A., King, R.W., McClusky, S.C., Floyd, M., Wang, L., Murray, M., Melbourne, T.,Santillan, M., Szeliga, W., Phillips, D., Puskas, C.: Plate Boundary Observatory and Related Networks: GPS Data Analysis Methods and Geodetic Products. Rev. Geophys.,54, https://doi.org/10.1002/2016RG000529, 2016.

Hosking, J. R. M.: Fractional differencing. Biometrika, 68, 165-176, https://doi.org/10.1093/biomet/68.1.165, 1981.

Kasdin, N.: Discrete simulation of colored noise and stochastic processes and $1/f^{\alpha}$ power-law noise generation. Proc. IEEE, 83, https://doi.org/10.1109/5.381848, 1995.

Li, J., Miyashita, K., Kato, T., Miyazaki, S.: GPS time series modeling by autoregressive moving average method: Application to the crustal deformation in central Japan. Earth Planet Space, 52, 155-162, 2000.

Lilly, J.M., Sykulski, A.M., Early, J. J., and Olhede, S. C.: Fractional Brownian motion, the Matérn process, and stochastic modeling of turbulent dispersion. Nonlin. Processes Geophys. 24, 481–514, https://doi.org/10.5194/npg-24-481-2017, 2017.

Montillet, J.-P., Williams, S.D.P., Koulali, A., McClusky, S.C.: Estimation of offsets in GPS time-series and application to the detection of earthquake deformation in the far-field. Geophys. J. Int., 200(2), 1207-1221, https://doi.org/10.1093/gji/ggu473, 2015.

Montillet, J.-P., and Bos, M.S.: Geodetic Time Series Analysis in Earth Sciences. Springer Geophysics, https://doi.org/0.1007/978-3-030-21718-1, 2019.

Panas, E.: Estimating fractal dimension using stable distributions and exploring long memory through ARFIMA models in Athens Stock Exchange. Appl. Fin. Econ., 11(4), 395-402, https://doi.org/10.1080/096031001300313956, 2001.

Pipiras, V., Taqqu, M.: Long-Range Dependence and Self-Similarity. Cambridge Series in Statistical and Probabilistic Mathematics, Cambridge University Press (ISBN:9781139600347), 2017.

Samorodnitsky, G., and Taqqu, M. S.: Stable Non-Gaussian Random Processes: Stochastic Models with Infinite Variance (Chapman and Hall, London), 1994.

Taqqu, M.S., Teverovsky, V., Willinger, W.: Estimators for long-range dependence: an empirical study. Fractals, 3(4), 785-798, https://doi.org/10.1142/S0218348X95000692, 1995.

Tregoning, P., Watson, C.: Atmospheric effects and spurious signals in GPS analyses. J. Geophys. Res., 114 (B09403), https://doi.org/10.1029/2009JB006344, 2009.

Weron, A., Burnecki, K., Mercik, S., and Weron, K.: Complete description of all self-similar models driven by Levy stable noise. Phys. Rev. E., 71, 016113, https://doi.org/ 10.1103/PhysRevE.71.016113, 2005.

Williams, S.D.P.: The effect of coloured noise on the uncertainties of rates estimated from geodetic time series. J. Geod., 76, 483-494, https://doi.org/10.1007/s00190-002-0283-4, 2003.

Williams, S.D.P., Bock, Y., Fang, P., Jamason, P., Nikolaidis, R.M., Prawirodirdjo, L., Miller, M., Johnson, D.J.: Error analysis of continuous GPS position time series. J. Geophys. Res., 109(B03412), https://doi.org/10.1029/2003JB002741, 2004.